A formal framework for the representation of stack-based terrains

Article *in* International Journal of Geographical Information Science · May 2018

DOI: 10.1080/13658816.2018.1475671

CITATIONS
4

READS
249

3 authors:

Alejandro Graciano Segura
Universidad de Jaén
7 PUBLICATIONS **64** CITATIONS
SEE PROFILE

Antonio J. Rueda
Universidad de Jaén
50 PUBLICATIONS **464** CITATIONS
SEE PROFILE

Francisco R. Feito
Universidad de Jaén
169 PUBLICATIONS **1,547** CITATIONS
SEE PROFILE

A formal framework for the representation of stack-based terrains

Alejandro Graciano[a], Antonio J. Rueda[a] and Francisco R. Feito[a]

[a]Department of Computer Science, University of Jaén

ARTICLE HISTORY
Compiled January 9, 2024

ABSTRACT
The definition of formal frameworks in GIScience is important for the assessment of spatial data representations, the study of their properties and the design of efficient and robust algorithms. This paper describes a formalization for the representation of 3-dimensional geological models as well as the adaptation of several spatial operations for common GIS fields to this representation. We use the Stack-Based Representation of Terrains (SBRT) in order to model volumetric structures, both at surface and subsurface levels, thus preventing the large storage requirements of regular voxel models. Furthermore, we base our work on the geo-atom theory in order to provide our framework with a solid formal geographic foundation. This paper covers both conceptual and implementation levels of the framework. In the conceptual level the mathematical foundations for the representation of the stack-based representation, their connection with the geo-atom theory and the derived operations are depicted. Then, a data model and an implementation extending the coverage concept provided by the GML standard are suggested.

KEYWORDS
Stack-based representation; Terrain modelling; Raster data modelling; 3D modelling

1. Introduction

Advances in data acquisition technologies have resulted in a vast amount of spatial data valuable for geoscientific and geoinformation-related fields (Guo *et al.* 2016). Most of this data is obtained from scanning surveys using laser techniques, such as LiDAR systems, (Cacciari and Futai 2017, Mitasova *et al.* 2012) or physical techniques, like electromagnetic methods (Abedi *et al.* 2012), which provide accurate geological models of terrains at surface and subsurface levels. The way this data is represented in a computer is crucial for its efficient management, processing and visualization. Therefore, the study of spatial data representations has been a key point in GIS and geoscientific research in the last decades (Thiele *et al.* 2016, Wang *et al.* 2016).

This is an Accepted Manuscript of an article published by Taylor & Francis in International Journal of Geographical Information Science on May 2018, available at: http://dx.doi.org/10.1080/13658816.2018.1475671

Corresponding author: Alejandro Graciano. Email: graciano@ujaen.es

The traditional ways of representing surface terrain is by means of height maps, or voxel models when a representation of volumetric surface features and/or subsurface structures is required. An integral and efficient solution for both cases is using a hybrid strategy: instead of storing a single value for each cell in a regular grid, a list of intervals is stored in what is called a materials stack. Each stack compacts a vertical sequence of voxels with a common material or physical property, and can be seen as a representation of the data generated from a borehole logging (Figure 1). This representation, called the Stack-Based Representation of Terrains (SBRT), was originally introduced by Benes and Forsbach (2001) for the simulation of erosion processes in 3D terrains, and has since proven its usefulness in numerous subsequent papers (Peytavie *et al.* 2009, Löffler *et al.* 2011, Natali *et al.* 2014).

Our purpose here is to define a formal framework to validate this representation and define properties and algorithms precisely. There are formal frameworks that cover the definition both of discrete object models (implemented as vector data models in GIS) (Molenaar 1992, Yu *et al.* 2016) and continuous fields models (implemented as raster data models) (Tomlin 1990, Kjenstad 2013) but in an isolated way. Nevertheless, there are many scenarios which require a general or hybrid representation that deals at the same time with both data types. In the early 1990's, Goodchild already pointed out the necessity to unify both data models in a general spatial representation, introducing for this purpose the geo-atom theory (Goodchild 1992).

Our formal framework for the stack-based representation of terrains is based on the geo-atom theory. This formalism is completed by describing a set of relevant operations that provide value to the system. Due to the abstraction provided by the geo-atom theory, the framework is able to deal not only with a 3D distribution of geological materials or volumetric surface features, but with any other physical or environmental property useful for terrain analysis or simulation. Therefore, the proposed framework aims to support geoscientists with a simple and well-defined model for 3D terrain and subsurface modeling.

2. Previous work

2.1. *Formal spatial models*

Formal models have played a major role in the geographic information sciences and geoscientific evolution, from the first systems which only considered 2D data (Longley *et al.* 2015) to the new general frameworks for the representation of nDimensional objects (Karimipour *et al.* 2010, Arroyo Ohori *et al.* 2015). One of the first geospatial issues addressed by the definition of formal models was the spatial relations among discrete objects such as topological, order or metric relations (Egenhofer and Franzosa 1991). Many were the theoretical models and data structures proposed for this purpose. For example, Molenaar (1990) suggested one of the first data structures that validated this type of relations for three-dimensional data: the 3D Formal Data Structure (3D FDS). 3D FDS defines nodes, edges and arcs as basic elements, that can be combined into surfaces and bodies as higher level objects. This work was continued by Zlatanova (2000) by proposing a formal model focused on the improvement of spatial queries and by Coors (2003) who introduced an urban model from 3D FDS among others.

Several approaches are based on the mathematical formulation of the cell and simplicial complexes theory. A simplex or n-simplex is the convex hull of $n + 1$ points in a Euclidean space of dimension less than n. Hence, a 0-simplex is a node, a 1-simplex

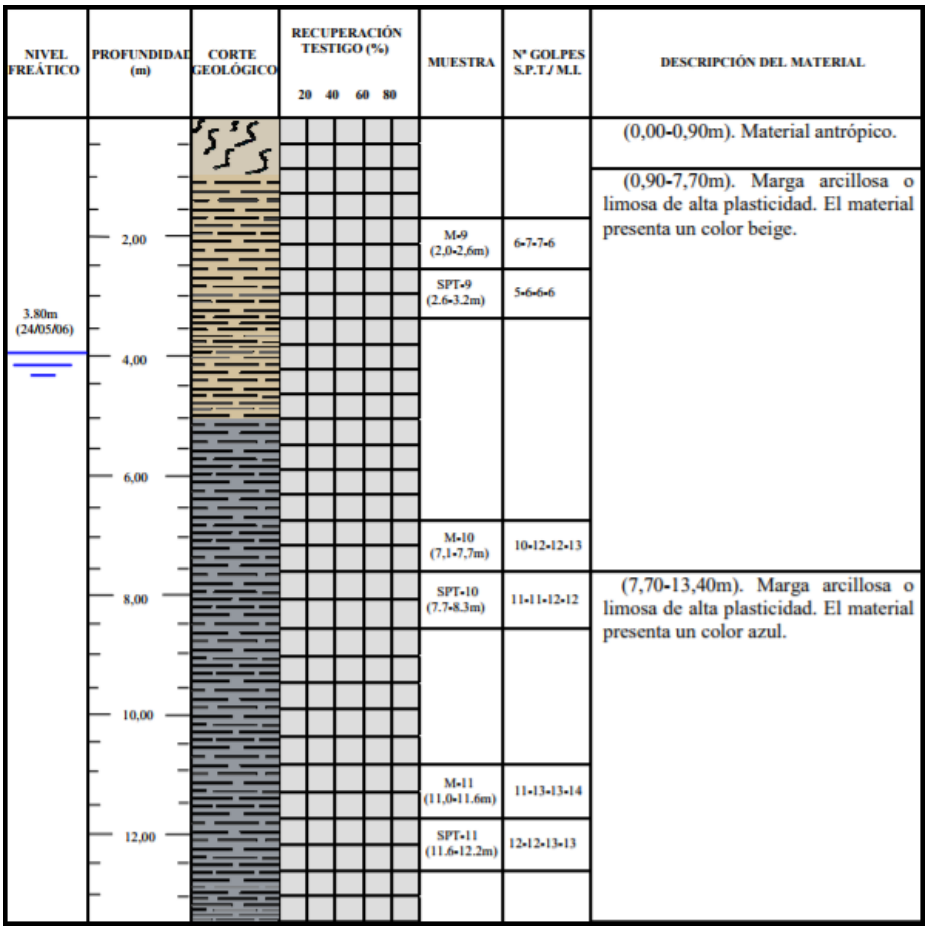

Figure 1. A real example of borehole log extracted from a geotechnical survey of the subsurface of the University of Jaén (Spain)

is an edge or arc, a 2-simplex is a triangle and a 3-simplex is a tetrahedron. The combination of them forms more complex objects. Examples include its adaptation to a graph structure presented by Brisson (1993), the work of Pilouk (1996) who proposed the TEtrahedral Network (TEN) to solve some difficulties in modeling objects with unclear boundaries, and its extension in combination with Morse theory (Forman 1998, Luricich and De Floriani 2014, De Floriani *et al.* 2015). Generalized maps (G-maps) are similar to the graph proposed by Briston and they have been applied to the explicit representation of the topology from a hierarchical partitioning of the objects (Le *et al.* 2013). B-Rep and simplicial complexes are also widely used in computer graphics for solid modeling (Hughes *et al.* 1990, Čomić *et al.* 2014).

Topological relationships have also been modeled with the 9-intersection model (Egenhofer 1989). This model describes these relationships with a matrix which is capable of representing the eight possible spatial relations between two objects: disjoint, meet, contain, inside, cover, coverby, equal and overlap (de la Losa and Cervelle 1999, Billen and Zlatanova 2003, Borrmann and Rank 2009, Wang *et al.* 2016). Other formal frameworks for discrete objects are focused on geometric algebra (Yuan *et al.* 2012, 2014) or use an object-oriented strategy (Shi *et al.* 2003).

The previous works show examples of formal models for discrete objects. In dealing with continuous domains, it is first necessary to discretize the space. The most common form of discretization is a regular grid of cells. Map algebra (Tomlin 1990) is the most widely used formalism for the definition of operations on grids. This algebra consists of a set of map layers as operands and a set of arithmetic, logical or relational operations. Due to its simplicity and power, map algebra has become a *de facto* standard for raster management in GIS (GRASS Development Team 2016, ESRI. Environmental Systems Research Institute 2017). Also, this framework has been used in geoscientific problems such as the calculation of network flow direction (She and Li 2016) or in modeling components for environmental systems (Schmitz *et al.* 2013, Rueda *et al.* 2013).

Map algebra was originally introduced for the 2D domain. An evident improvement is to extend this framework to a 3D space and therefore, use voxel models as operands. Mennis *et al.* (2005) benefited from this additional dimension to handle spatio-temporal models. Likewise, in order to obtain dynamic models, Takeyama and Couclelis (1997) merged map algebra with cellular automata developing the geo-algebra generalization. But map algebra operations can be defined not only on regular grids. Ledoux and Gold (2008) suggest that Voronoi diagrams can be used in combination with map algebra for modeling 3D geoscientific fields. A more general framework was proposed by Kjenstad (2013) in which the concept of hyperfields or field-of-field structure was introduced.

However, many problems consider both discrete objects and continuous fields (Brooks and Whalley 2008, Wang *et al.* 2010). In order to deal with them, it has been proposed, on the one hand, to perform conversions between the different data (Shen *et al.* 2013) or, on the other hand, to define a more general framework that integrates both approaches in a hybrid one. Regarding the latter, the theory presented by Goodchild *et al.* (Goodchild *et al.* 1999, 2007) is still subject of research: in the paper presented by Jjumba and Dragićević (2015) voxel automata are used together with geo-atoms for the simulation of geospatial processes. Extending this theory, Wang *et al.* (2015) developed a formal framework for the modeling of movement, and Voudouris (2010) a general framework of fields to deal with uncertainty. Recently, Zhu *et al.* (2017) have underscored the limitations of geo-dipoles for covering spatial patterns for multiple locations, exposing some examples in which statistics operations require a more general approach.

2.2. *Terrain modeling*

Terrain modeling is a key feature in geoscientific applications but has also applications in videogames, simulators or special effects in films. As we stated before, subsurface and volumetric data are usually modeled by means of voxel models (Hollt *et al.* 2012, Watson *et al.* 2015), however there are approaches that explore the possibilities of several of the data models and frameworks described in the previous section. In (Lemon and Jones 2003) it was proposed a geological model in which the separation among the various strata was represented using triangular surfaces or TINs. Regarding TEN representation, Penninga and Van Oosterom (2008) introduced a new data structure that modeled both surface and subsurface spatial datasets, partitioning the 3D space into a set of connected 3-simplexes. Caumon *et al.* (2012) used tetrahedral meshes for gathering data from different sources such as remote sensing images and DEMs, resolving the generated discontinuities. The verification of the topology in this kind of data structures can be highly complex, therefore hierarchical data structures (Crespin *et al.* 2014) and other representations focused on the assessment of the topological relations have emerged (Wu 2004). Furthermore, methods for the generation of geological subsurface models based on these representations using finite elements (de Oliveira Miranda *et al.* 2014) or using GPU computing (Mateo Lázaro *et al.* 2014) have also been presented.

In reference to surface modeling, there have been introduced approaches focusing on hierarchical data structures (Yalçin *et al.* 2011, Noguera *et al.* 2011). Other examples are the work of Hnaidi *et al.* (2010) which used diffusion equations in order to generate landscapes from parametrized curves, or the workflow for the deformation of surfaces proposed by Maxelon *et al.* (2009) among many others. Nevertheless, these approaches cannot model volumetric features in the surface like caves, natural arcs or cliffs. In order to overcome this limitation, several papers that used the SBRT (Peytavie *et al.* 2009, Löffler *et al.* 2011), Gmaps (Crespin *et al.* 2014), or hybrid systems, by combining CSG modeling, shape grammars and morphing (Zawadzki *et al.* 2012), or combining traditional voxel models and height maps (Koca and Güdükbay 2014) have been presented.

3. Modeling 3D terrains

This section describes the formalization of the stack-based representation of terrains as well as the theoretical background in which our approach is sustained. Our work is based on the concepts of geo-atom (Goodchild *et al.* 1999) and geo-dipole (Goodchild *et al.* 2007), which were presented as primitives for the representation of geographic information.

3.1. *Concepts of Geo-atom theory*

A geo-atom is a tuple $< \mathbf{p}, Z, z(\mathbf{p}) >$ which contains information about the value ($z(\mathbf{p})$) of a property (Z) at a specific position ($\mathbf{p}$). A property and the set of possible values that can be obtained are sometimes referred to as the domain and its range respectively. The dimensionality of $\mathbf{p}$ is not limited to any space, therefore, a 3D space or 4D space-time are suitable to be adopted.

Geo-atoms are assembled into geo-objects or geo-fields depending on the type of information provided. Geographic data like points, lines, polygons or solids are repre-

sented as geo-objects, while geo-fields are the aggregations of geo-atoms over a space-discretized domain. These are commonly identified with vector and raster logical models respectively.

The possible discretizations for a geo-field can be categorized into two groups: Tessellation-Based Geo-Fields (TBGF) and Sampled and Interpolated-Based Geo-Fields (S&IBGF) (Liu *et al.* 2008). In TBGF the sampling value obtained from a position within a domain is the value associated to the tile identified at this position. In other words, all the geo-atoms contained in a tile have the same property value. A remote sensing image which characterizes coastal zones (discretized as a regular grid of pixels) is an example of a TBGF. On the other hand, a S&IBGF uses some kind of interpolation to sample a value from a specific position. For instance, in order to retrieve the height from a 2D position in a digital elevation model (using a regular 2D array of points as discretization as exposed in Table 1), an interpolation value is computed using the nearest sampling points. The most common approaches of discretization, identified by Goodchild *et al.* (2007), are shown in Table 1. These approaches were introduced for a 2D domain to the best of our knowledge; nevertheless they can be extended to any dimension.

Table 1. Common discretizations for geo-fields

Discretization	Type	Objects discretized	Example
F1	TBGF	Non-overlapping polygons	Choropleth map
F2	TBGF	Triangular elements	Triangular Irregular Networks
F3	TBGF	Regular grid of cell	Digital Elevation Models
F4	S&IBGF	Irregular spaced points	LiDAR data
F5	S&IBGF	Points in a regular array	Air Pollution
F6	S&IBGF	Isolines	Topographic Maps

Geo-atoms can describe all the spatial phenomena for isolated locations such as pollution level or river networks. However, many properties need the interaction among locations.

In contrast with a geo-atom which links a property to a location, a geo-dipole links two locations ($\mathbf{p_1}$ and $\mathbf{p_2}$), a new property (Z) and the value of applying the property to the pair of locations ($z(\mathbf{p_1}, \mathbf{p_2})$). The interaction is summed up by the tuple $< \mathbf{p_1}, \mathbf{p_2}, Z, z(\mathbf{p_1}, \mathbf{p_2}) >$ (Zhu *et al.* 2017). Geo-dipoles are quite useful for terrain modeling. There are several properties very common in geoscientific applications which require a connection between locations. Problems like viewshed analysis (Zhao *et al.* 2013), drainage network determination (Ortega and Rueda 2010) or the assessment of optimal flood protection levels in urban flood risk management (Wang *et al.* 2010) can be accomplished with the use of geo-dipoles. For example, given a visibility property for a terrain surface that indicates whether a location $\mathbf{p_1}$ is visible from another location $\mathbf{p_2}$, the geo-dipole for each point is $< \mathbf{p_1}, \mathbf{p_2}, is\_visible, true >$. Geo-dipoles provide a generalization to several interaction models proposed in the literature, namely object fields (Cova and Goodchild 2002), metamaps (Takeyama 1997), object pairs (Goodchild 1992) and association classes (Zeiler 1999).

From these models, the concept provided by object fields is especially relevant for our framework. In a object field each point maps not to a value but to a geo-object with the set of locations which meet a property given by a specific geo-dipole. This is interesting since many geoscientific and GIS problems do the gathering or an analysis of a set of locations that fulfill a requirement. Taking the example of the visibility

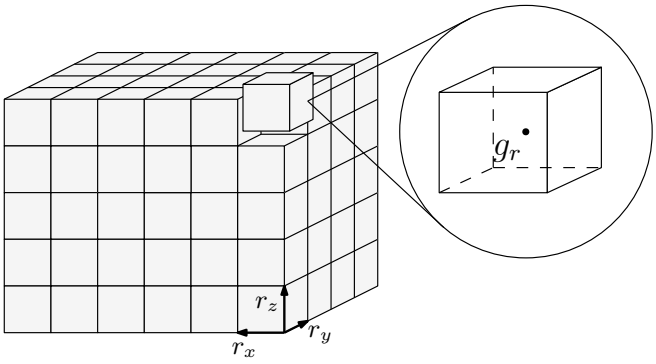

Figure 2. Relation between a 3D regular grid and a representative geo-atom

property again, a geo-object $O(\mathbf{p_1})$ can be generated with all the locations that are visible from $\mathbf{p_1}$. This concept is also valid for a neighborhood since we can construct a geo-object with the locations of those geo-atoms that are within an area of influence.

3.2. *Terrains as geo-fields*

Most of the properties that can be measured in a terrain are continuous (e.g., material distribution, terrain resistivity or erodibility) and therefore, can be represented with a geo-field. Since a geo-field can aggregate an infinite set of geo-atoms, it is necessary to define a discretization scheme in order to simplify and make the representation manageable.

In terrain and geological modeling one of the properties that can be sampled in a geo-field is the material at a specific position. This property can be mapped by a scalar TBGF that establishes the aggregation of a set of geo-atoms characterized as:

$$< \mathbf{p}, M, f_m(\mathbf{p}) >$$

where $M = \{m_0, m_1, m_2, \ldots, m_n, u\}$ is the set of materials sampled (e.g., sand, clay, air, etc.), u the material classified as unknown, $\mathbf{p} \in \mathbb{R}^3$ is a space location and f_m a surjective function defined as:

$$f_m : \mathbb{R}^3 \rightarrow M$$

There exists many ways to discretize a geo-field for terrain and subsurface modeling. The space discretization most commonly used is a 3D regular grid or voxel model in a 3D extension of the F3 type (Table 1). Then, given a grid with dimensions $h \times w \times d$ and resolution $r = (r_x, r_y, r_z)$, each point maps to a voxel unambiguously. For each voxel it can be defined a *representative* geo-atom g_r. This geo-atom serves as input in several of the operations in our framework and may be located at any point of the voxel. In our case we set g_r as the centroid of the voxel (Figure 2).

A space tessellation as a regular grid is a straightforward way to conceptualize geo-fields but it can lead to implementations with high memory requirements. For that reason in the next section; we propose a more compact representation: the stack-based representation of terrains (Graciano *et al.* 2017).

3.3. *Stack-based representation of terrains*

From a conceptual point of view, the stack-based representation of terrains can be seen both as an extension of a Digital Elevation Model (DEM) and a compressed representation of a voxel model. DEMs are limited to a single height value for each grid cell; therefore, it is unsuitable for representing some geological features such as aquifers, caves or overhangs. Instead, a SBRT stores for each cell a series of heights in conjunction with a property in form of intervals. Our representation differs from standard voxel-based model in which each interval is a set of packed voxels with a common property or attribute value and the same x, y coordinates. The intervals can be denoted as tuples $< m, h >$, where h corresponds with the maximum height of the interval and $m \in M$ with its material.

In contrast with voxel models, a SBRT discretizes the xy plane in a 2D regular grid whereas the compressed voxels are represented as a non-regular grid along the z coordinate. In this way, the minimal sampling elements (the intervals or *cuboids* due to their geometric shape) are organized in *stacks* along the z direction. Given the set of voxels packed by an interval, its $g_r =< p, M, f_m(p) >$ is the representative geo-atom of the upper voxel. Therefore, in the tuple $< m, h >$ defined above, m corresponds with $f_m(p)$, and the maximum height of the interval, h, is determined by $p.z$ and the resolution of the 3D regular grid in the z direction, i.e., $h = p.z + r_z/2$. As a result, in order to compute the function f_m from a 3D position, it is necessary to select a stack from the x, y coordinate to finally obtain the corresponding interval of the stack from the z coordinate. More formally, given a 3D position (x, y, z), we calculate $f_m(x, y, z)$ as follows. Firstly, a stack S must be selected from the (x, y) coordinates. S have to verify $|p_x - x| < r_x/2$ and $|p_y - y| <= r_y/2$, where p is the location of any of the representative geo-atoms of its intervals. S is a set of intervals $S = \{I_1, I_2, I_3, \ldots, I_n\}$ sorted by their representative geo-atoms height in ascending order. Therefore, $f_m(x, y, z) = m_i$, being i the index of the interval that verifies $h_{i-1} < z \leq h_i$, with $i > 1$, or m_1 in the case of $h_{min} < z < h_1$, being h_{min} the z coordinate of the bottom face of the cuboid I_1. Otherwise, $f_m(x, y, z) = u$.

Following this, a SBRT geo-field can be seen as an aggregation of two geo-fields at different levels, forming a hyperfield (Kjenstad 2013). The higher level geo-field, which represents the grid of the terrain, follows a discretization of type F3. Regarding the lower level geo-fields, namely the set of stacks, they are defined as an irregular but geometrically shaped tessellation, according with an F1 discretization. Figure 3 shows an example of a 3D terrain modeled by voxel data, the resulting DEM and a stack of intervals. Our framework can be seen in the context of geo-atom theory in Figure 4.

So far, SBRT has been mainly used in fields other than GIS. Benes and Forsbach introduced this concept for managing the simulation of thermal erosion in terrains (Benes and Forsbach 2001). Peytavie *et al.* (2009) used this structure for the rendering of realistic 3D terrain models allowing the modeling of caves o arches. The surface of these elements was generated from an implicit model, and SBRT is only used as an intermediate representation. This work was improved by decreasing the required time in the terrain generation procedure (Löffler *et al.* 2011). Natali *et al.* (2014) adopted this scheme for modeling both surface and subsurface structures in an application for sketching geological features. This application was designed to help geologists to teach geological concepts such as strata layers, lakes, or rivers.

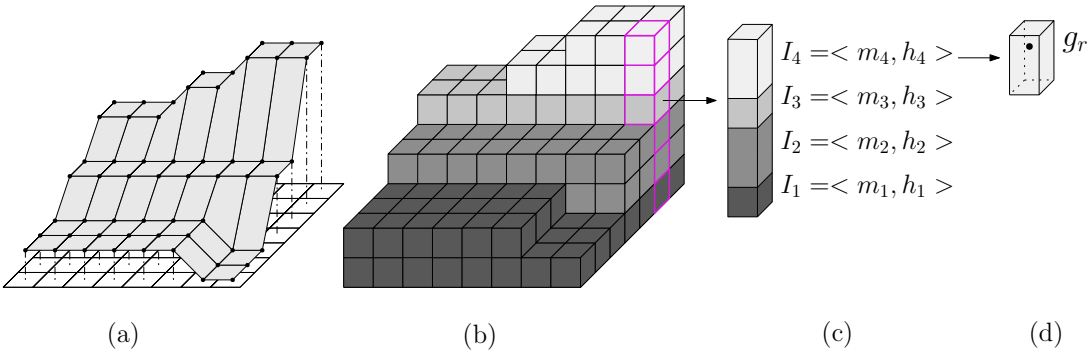

Figure 3. Example of a 3D terrain model with the stack-based representation (b). A DEM of the terrain is showed (a), a sample stack (c) and an interval (d) are also represented.

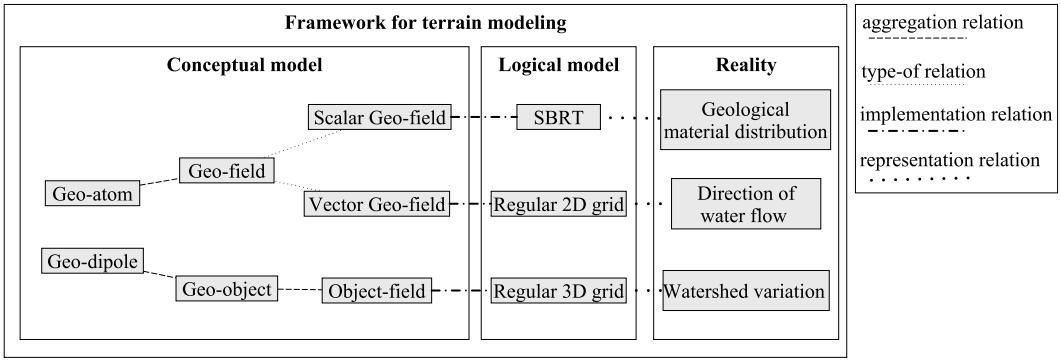

Figure 4. Stack-based representation of terrains in the context of geo-atom theory

4. Operations with 3D terrains

Once SBRT has been described, this section focuses on the characterization of common operations for his representation.

GIS and many geoscientific applications commonly require operations such as feature clipping or intersection, buffering, scale change, format conversion, distance measurement and so on. One of the reasons why researchers make efforts to improve the way in which spatial data is represented is to implement these operations in an efficient way. Traditionally, many manipulation and spatial analysis operations for fields have been defined by means of map algebra (Tomlin 1990). This framework, inspired by the methods of Image Processing (Ritter *et al.* 1990), classifies spatial operations depending on their context. Initially three kinds of operations were defined: local, focal and zonal.

In local operations (1) each cell of the new map layer is created from the gathering of overlapping isolated cells of the input layers. Consequently, regarding the number of operands, local operations can be unary as well as n-ary operations. In contrast, in a focal operation (2) on a position **p**, the output cell is computed from an input cell in that position and its neighborhood from the input layers. Usually the neighborhood is based on pixel adjacency in a similar way to image convolution. Finally, in zonal operations (3) each output cell is computed from a zone of a unary input layer in a similar approach to focal operations. The zones of the input layer must be non-overlapping, therefore a cell only belongs to a single zone. Every output cell within an input zone is provided with the same value, which is the result of the aggregation of the cells inside the zone.

In addition to these operations, some authors have included global operations. These unary operations are performed on an entire layer. For instance, algorithms based on distances, such as least cost path or geometric conversions can be considered as belonging to this category (DeMers 2002).

Liu et al (Liu *et al.* 2008) for their general field conceptualization extended the map algebra operations by reformulating some of them and adding new ones. For instance, local operations were separated, depending on the number of input layers, into *reclassification* operations and *overlay* operations for unary and n-ary operations respectively. Also, they defined the *subset* (or *slice*) and *object identification* operations which can be used for extracting some part of a layer. In addition an operation for the application of a *generalization* or level of detail was described.

The previous operations are irreversible since an input layer cannot be obtained from its output. The authors denoted this type of operations as Order-Increasing Operations (OIOs); otherwise they are Non-OIO (NOIO). Operations such as geometrical transformations, exact interpolation and Fourier transformations are examples of the latter.

4.1. *Definition of operations*

Although map algebra was designed taking into account 2D raster layers, its principles can be extended to the SBRT. However, not all operations can make sense. Subset and object identification have the same meaning for a SBRT and therefore can be combined into a single operation. Moreover, an exact interpolation operation is obviously not appropriate because a SBRT is defined by a TBGF model. Likewise, a Fourier transformation does not seem to match with our model since it is not an image. Table

2 gives some examples of possible operations for each type, while Table 3 illustrates each operation of map algebra on SBRTs.

Table 2. Examples of SBRT operations

Operation type	Example	Output geo-field	Order
Reclassification	Binarization	Scalar TBGF	OIO
Overlay	Boolean Union	Scalar TBGF	OIO
Focal operation	Normal surface calculation	Vector S&IBGF	OIO
Zonal operation	Material percentage calculation	Scalar TBGF	OIO
Global operation	Euclidean distance to a position	Scalar/Vector S&IBGF	OIO
Subset operation	Cross section extraction	Scalar TBGF	OIO
Object identification	Material layer removal	Scalar TBGF	OIO
Generalization	Level of detail	Scalar TBGF	OIO
Geometrical transformation	Coordinate system conversion	Scalar TBGF	NOIO

In map algebra and its subsequent developments (Cordeiro *et al.* 2009, Schmitz *et al.* 2013), the operations receive as inputs a layer (unary operation) or a set of layers (n-ary operation) although the actual computed elements are the individual map cells values. In 3D map algebra (Mennis *et al.* 2005), the computable elements are the voxels values. Accordingly, in our framework the input elements of the operations are the elements contained in the intervals, i.e., the geo-atoms / geo-dipoles / geo-objects. For the sake of simplicity, we define and give examples of just unary and binary operations.

First of all, in order that a couple of intervals can be computed in a binary operation, the input geo-fields must be spatially congruent. This requirement is divided into two constraints:

(1) The SBRT geo-fields must be congruent at grid cell level. This means that the implied geo-fields should have the same grid resolution. If not, a generalization operation (see below) must be performed to the geo-field with larger resolution to avoid loss of precision. If required, a readjustment of the position of the grid can be carried out to make them fit perfectly.
(2) The SBRT geo-fields must be congruent at interval level. Operations between stacks have to be applied to couples of intervals with the same position and height. Two intervals can overlap in three different ways: (1) full match when both representative geo-atom position and height match, (2) partial match when only a part of both intervals overlap and (3) full inclusion when one of the intervals is entirely included in the other. Therefore, it is necessary *splitting* the intervals in the cases 2 and 3, in order to have the required full match before applying the operations.

An operation is specified by two components besides the input geo-fields: a function f that maps an input set into an output one and a position $\mathbf{p}$. The position is used for sampling the input set and also as output location. Thus, the operation can be described in tuple notation as $< f, \mathbf{p} >$.

The input set can be formed by a single property for most unary operations or by the product set of several properties in the case of binary operations. Some unary operations in which a single object field acts as input, for instance in focal operations, also use a product set.

The nature of the geo-fields can be very diverse depending on the type of the operation. The input and output sets do not have to be SBRT properties. For example, there are several operations that perform distance measurements or geometrical trans-

formations which use as input the set of locations. Hence, besides sampling materials or physical attributes among others SBRT properties, $\mathbf{p}$ can also be used to sample an input vector geo-field, an object-field or a geo-field that aggregates relations between geo-atoms in the form of geo-dipoles.

For the sake of illustration, several of the operations depicted in Tables 2 and 3 are described in detail below:

- **Binarization**. A change of the property measured in a location is referred as a reclassification of a geo-field. Due to the unary and local nature of the operation, it is performed for each interval in isolation. Therefore, the location $\mathbf{p}$ of the operation is the representative geo-atom of the interval and its function is defined by $f : Z_1 \rightarrow Z_2$ that takes the property of the input geo-field (Z_1) and map each interval to an output property (Z_2).

  A simple example for a geo-field representing a SBRT is the binarization of the materials: given the set of materials M, a function f can be defined as $f : M \rightarrow B$ where $B = \{solid, air\}$. The function maps to a binary *solid* value the materials *air* or *unknown*, and *solid* otherwise. The output position $\mathbf{p}$ is the position of the representative geo-atom belonging to the input interval.
- **Logical operations**. In contrast with reclassification operations, overlay operations require a set of spatially congruent geo-fields as input in order to perform them. In this case, the function is defined by $f : Z_1 \times Z_2 \rightarrow Z_3$.

  Logical operations are a typical example in map algebra. Let us define a terrain subsurface dataset and a groundwater dataset, both geo-fields represented by a SBRT. Assuming that both layers are overlapped and congruent in space, they can be combined into a single geo-field by using a logical operation. In this case, a splitting operation has to be performed over pairs of stacks. Once the geo-fields are totally congruent the operation can be computed. The transition function $f : M_1 \times M_2 \rightarrow M_3$ with $M_3 = M_1 \cup M_2$ where $M_1 = \{air, ground, u\}$ and $M_2 = \{water, u\}$, can be defined with the conditional rule:

$$f(m_1, m_2) = \begin{cases} m_2, & \text{if } m_2 = water \\ m_1, & \text{otherwise} \end{cases}$$

  With $m_1 \in M_1$ and $m_2 \in M_2$. Finally, the location of the operation is the representative geo-atom of the interval once the splitting operation is applied.
- **Convolution operations**. During the computation of an operation of this type at a specific position, it is necessary a sampling of the neighbor locations in order to obtain the final value, i.e., a focal operation must be applied at every location $\mathbf{p}$. For each location a geo-atom or a geo-dipole (if an interaction between the actual and neighbor locations is required) is generated with the new sampled value. Their locations can be gathered in a geo-object $O(\mathbf{p})$ that forms a geo-field in which a location maps to a geo-object. These geo-objects are the input for the function $f : Z_1 \times Z_1 \times \cdots \times Z_1 \rightarrow Z_2$.

  The computation of the normal vector of an isosurface is an illustrative example of this kind of operation. This is a common operation for both terrain analysis (for instance, for slope or drainage network calculation) and visualization purposes. In this context, we define an isosurface as the set of face portions of the cuboids associated with the intervals, which are in contact with a given material (called isomaterial). A normal vector can therefore be computed at each

Table 3. A conceptual view of the operations of the SBRT

Input(s)	Output	Function
Reclassification		
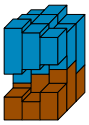	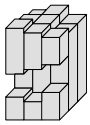	$f : M_1 \rightarrow M_2$
$M_1 = \{m_1, m_2, m_3, u\}$	$M_2 = \{m_4, u\}$	
Overlay		
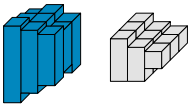	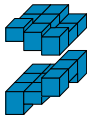	$f : M_1 \times M_2 \rightarrow M_1$
$M_1 = \{m_1, u\}$ $M_2 = \{m_2, u\}$	$M_1 = \{m_1, u\}$	
Focal operation		
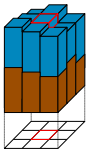		$f : M_1 \times \cdots \times M_1 \rightarrow M_1$
$M_1 = \{m_1, m_2, m_3, u\}$		
Zonal operation		
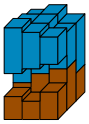		$f : M_1 \times \cdots \times M_1 \rightarrow M_2$
$M_1 = \{m_1, m_2, m_3, u\}$	$M_2 = [0, 100]$	
Global operation		
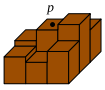		$f : M_1 \rightarrow M_2$
$M_1 = \mathbb{R}^3$	$M_2 = \mathbb{R}$	
Subset operation		
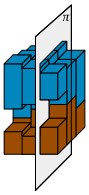		$f : M_1 \rightarrow M_2$
$M_1 = \mathbb{R}^3$	$M_2 = \{m_1, m_2, m_3, u\}$	

Table 4. *

Table 3 (continuation)

Input(s)	Output	Function
Object identification		
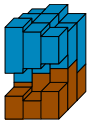		$f : M_1 \to M_2$
$M_1 = \{m_1, m_2, m_3, u\}$	$M_2 = \{m_2, u\}$	
Generalization		
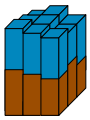	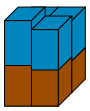	$f : M_1 \times \cdots \times M_1 \to M_1$
$M_1 = \{m_1, m_2, m_3, u\}$		
Geometrical transformation		
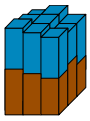	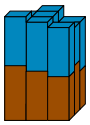	$f : M_1 \to M_1$
$M_1 = \mathbb{R}^3$		

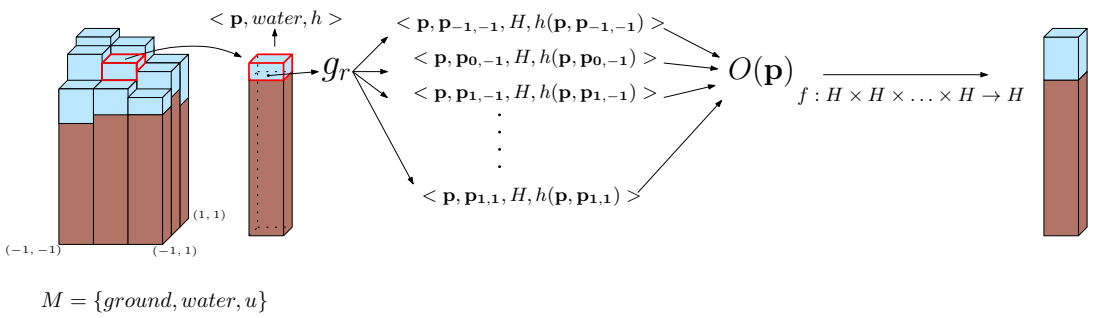

Figure 5. Computation of the water transfer to a stack from its neighborhood in a flooding algorithm.

point of this isosurface. In many applications it is common to use air or water as isomaterials; in these cases the vectors are perpendicular to the plane tangent to the ground at each point. For this operation, a 3D Moore neighborhood or kernel can be adopted, aligning the point to be processed with the kernel center. Both the cell size of the kernel and its dimension are setup values chosen depending on the desired accuracy of the method. For each neighbor $\mathbf{p_{i,j,k}}$ it is calculated a geo-dipole $< \mathbf{p}, \mathbf{p_{i,j,k}}, V, v(\mathbf{p}, \mathbf{p_{i,j,k}}) >$ where V is the property *unit vector* and $v(\mathbf{p}, \mathbf{p_{i,j,k}})$ the unit vector from $\mathbf{p}$ to $\mathbf{p_{i,j,k}}$. With the set of locations of those geo-dipoles that points towards an interval with the isomaterial, the geo-object $O(\mathbf{p})$ is formed, being the input of the function $f : V \times V \times \cdots \times V \to V$. The function calculates the normal vector to the surface as the sum of these geo-dipole values (unit vectors). Formally, this function can be described by the equation $f(f_m(\mathbf{p_{0,0,0}}), f_m(\mathbf{p_{0,0,1}}), f_m(\mathbf{p_{0,0,2}}) \cdots f_m(\mathbf{p_{n-1,n-1,n-1}})) = \sum_i \sum_j \sum_k v(\mathbf{p}, \mathbf{p_{i,j,k}})[f_m(\mathbf{p_{i,j,k}}) = isomaterial]$, being $n \times n \times n$ the dimension of the 3D kernel.

Another example is the calculation of drainage networks (Rueda *et al.* 2013). Given a SBRT geo-field constructed from a DEM ($M = \{ground, water, u\}$), a new interval can be added to each stack representing a water layer. Then, a flooding simulation is performed until the water of none of the intervals is transferred to the neighbor stacks. Formally, a stack at $(\mathbf{p_x}, \mathbf{p_y})$ location whose upper interval contains water, floods their neighbor stacks if its total height is higher. This procedure is repeated until a state of balance is reached. A flooding algorithm can receive as input a geo-object ($O(\mathbf{p})$) formed with a set of geo-dipoles indicating the difference of height (H) between an interval filled with water and located in $\mathbf{p}$ and its neighbors. The function is therefore defined by $f : H \times H \times \cdots \times H \to H$. Figure 5 depicts a step of this operation. Notice that in contrast with the original implementation described in (Rueda *et al.* 2013), an adaptation of the algorithm to SBRTs could also deal with underground water.

- **Level of detail**. The application of a generalization, also called Level of Detail (LoD), is a fundamental operation in GIS packages. It is required as a previous step for an n-ary operation as we stated before, but it also has applications as a compression method and for visualization. The result of this operation is a geo-field representing the same dataset but with a different cell resolution (only r_x and r_y are modified). The cells of the new grid can overlay one or more cells from the input grid. In the first case (the output cell overlies one single cell) the new cell will take as value the input stack. Otherwise, a splitting operation must be carried out with the overlapped cells in order to combine their stacks using, for instance, a weighted sum method.

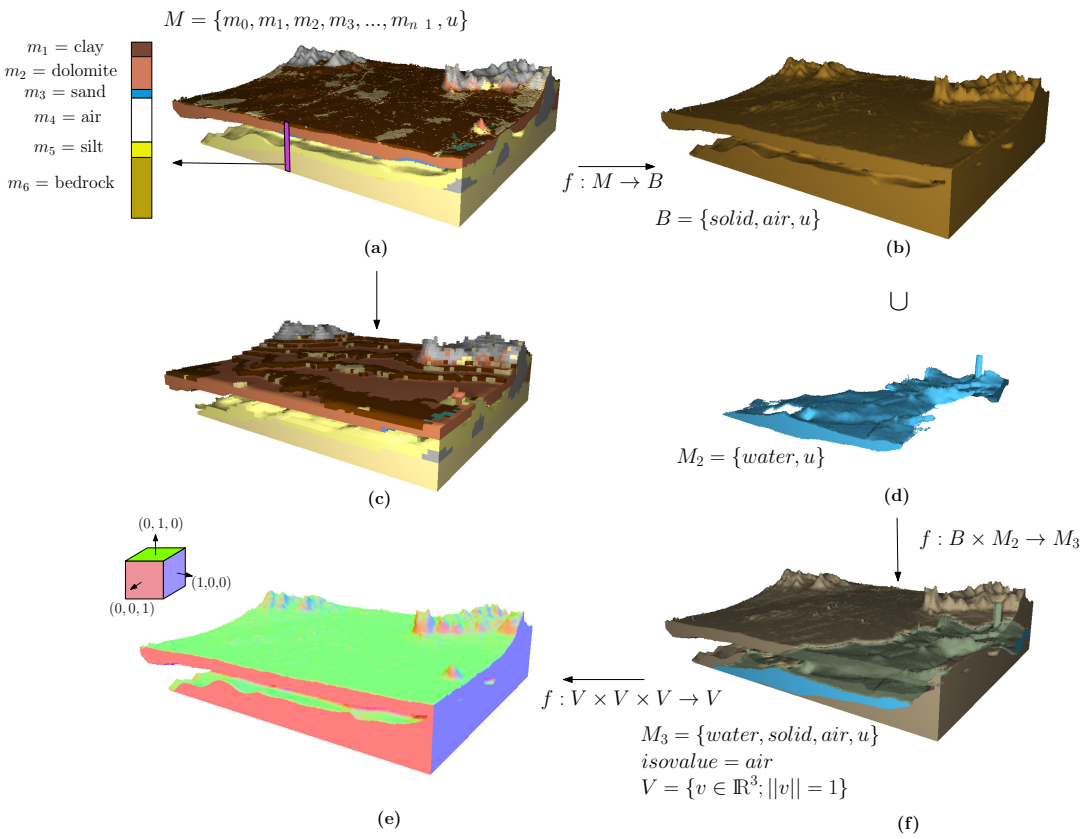

Figure 6. Examples of operations with a SBRT.

Figure 6 shows several examples of operations computed on a SBRT: an original SBRT geo-field (Figure 6.a) is reclassified to a binary SBRT (Figure 6.b) in order to indicate just *air* or *solid* material. Then, the result is taken as input of a logical operation in combination with a SBRT geo-field representing a subsurface aquifer (Figure 6.d). An attenuation of the *solid* material in the resulting geo-field (Figure 6.f) is shown to ease the visualization of the *water* material. The surface slope is then computed for this geo-field (Figure 6.e). Finally, the original geo-field is subjected to a generalization operation (Figure 6.c).

5. An implementation model

Section 4 gives a conceptual overview of the proposed representation for 3D terrains. In this section we provide an implementation based on the *de facto* standard Geography Markup Language (GML) (OGC 2007a).

The International Organization for Standardization (ISO) and the Open Geospatial Consortium (OGC) have collaborated in the creation of several geospatial standards such as the ISO 19107:2003 "Geographic Information - Spatial Schema" (OGC 2003), which provides the conceptual foundations previous to GML (ISO 19136:2007) or the ISO 19123:2005 "Geographic Information - Schema for Coverage Geometry and Functions" (OGC 2007b). The latter document defines the conceptual architecture for fields, referred to as *coverages*, and the implementation of this abstract specification by means of GML. We use the more recent proposal of coverage implementation (OGC

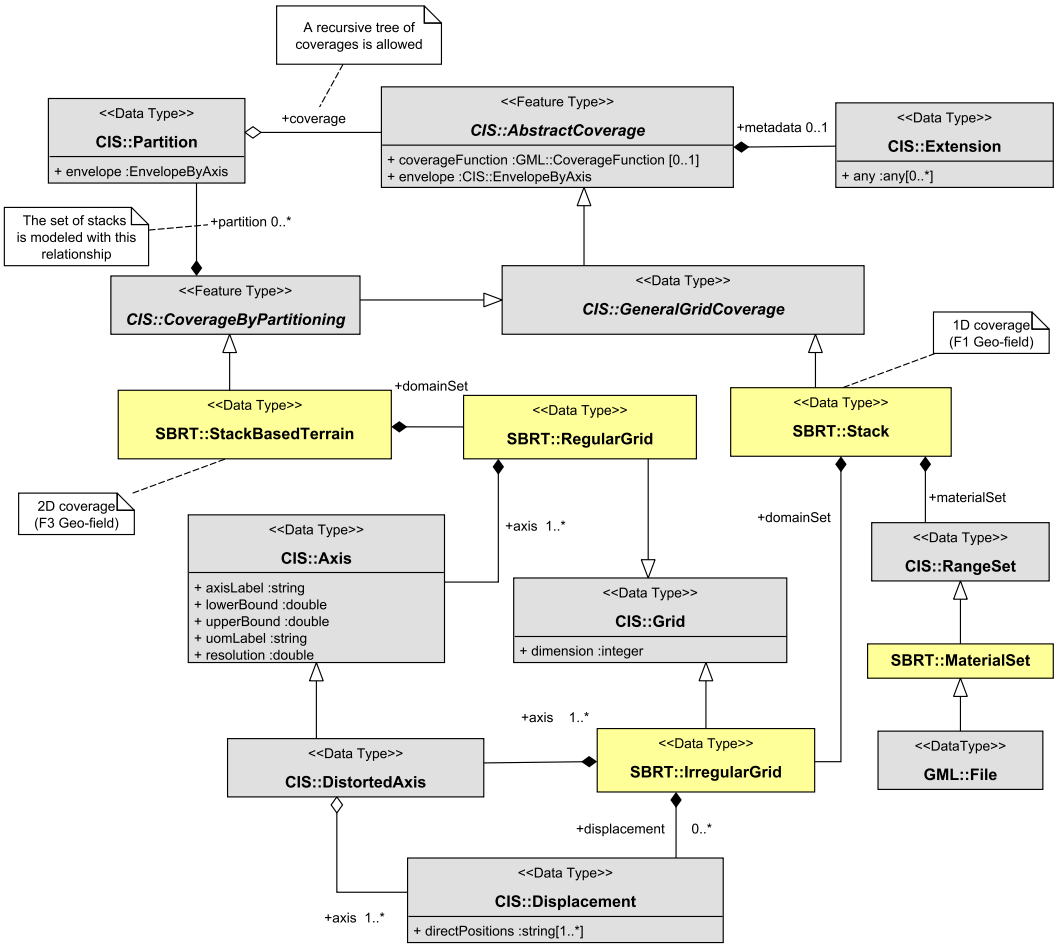

Figure 7. A simplified UML diagram depicting the main classes of an implementation of our framework

2015) rather than the original document because it fits better with the hyperfield concept (coverage partitioning). In addition, this Coverage Implementation Schema (CIS) adds some features to previous coverage specifications. For instance, it is not only XML-compliant, but it also considers an extension for a JSON encoding, which is planned to be included in future releases. Moreover, it provides new modeling capabilities, such as the addition of point cloud fields or a distinction between topological and geometric dimension of a grid.

Figure 7 shows a simplified UML diagram of a possible implementation of our framework using CIS and GML. Nodes in gray belong to GML/CIS framework, while yellow nodes are custom classes of our framework.

In contrast with the previous ISO/OGC coverage definition, CIS makes no distinction between discrete (TBGF) and continuous geo-fields (S&IBGF). They are modeled from the same data types; essentially with n-dimensional grids, set of points, curves or solids. A continuous coverage simply adds an interpolation method to its definition. The `CIS::AbstractCoverage` class is the core of CIS. This class models a geo-atom g by means of its *coverageFunction*. This function maps ($m(\mathbf{p})$) the elements of the domain set ($\mathbf{p}$) to those included in the range set (M). Actual instances of coverages such as regular or irregular grids, surfaces, solids or point clouds must be inherited

from this abstract class. Moreover, this class can include a set of metadata including descriptive information about the coverage.

In order to model the higher level geo-field of a SBRT (the 2D grid in the xy plane), we use the *coverage partitioning* feature in combination with a regular grid coverage (class `CIS::Grid`) which act as domain set. In the grid feature a Spatial Reference System (SRS) must be defined as well as the number of axes or dimensions, two in this case, and other axis-related data. Coverage partitioning has a set of sub-coverages which represent each stack of the terrain. Every partition must have the same or lower dimension than the main coverage. Our representation complies with this requirement since the stacks are one-dimensional. The actual lower level geo-field is modeled by an irregular grid through the `CIS::GeneralGridCoverage` class. In order to represent the intervals of the stacks, we use the `CIS::Displacement` class. This class models a partition in the grid axes by storing a sequence of the valid positions in this domain. Therefore, the relative positions of the intervals can be encoded in this class. Similarly to the previous field, the data regarding axes and dimension must be set for these fields.

Figure 8 shows a simplified encoding example of a naive SBRT in GML. The SBRT contains a 2×1 support grid with two intervals for each stack.

6. Conclusion and future work

Terrain modeling is a fundamental issue of many GIS and geoscientific applications. An efficient and extensible representation that is able to manage the large amount of spatial data retrieved by current acquisition technologies would be of great value to geoscientists. In this context, we have presented a formal framework for the representation of 3D terrains based on stacks. We have built our framework around the geo-atom theory, making use of many concepts like geo-dipoles, geo-fields, geo-objects and object-fields. We have explained why this scheme is more suitable for a complete terrain representation than voxel models and height maps, highlighting its computational efficiency.

Also, we have defined a set of operations for our system inspired by the well-known map algebra. Due to these sound foundations, many other high level operations like the removal of layers of materials or the calculation of a line-of-sight graph can be added to the framework in a straightforward way. In addition, we have suggested an example of how our representation can be implemented using a standard as GML.

In this paper, we have solely focused on field data type, and more specifically in 3D terrains. However, several geospatial problems require processing field and discrete data in a combined way. For example, engineering surveys may require terrain data modeled as a field as well as discrete objects representing pipelines or tunnels in order to perform a cost analysis. This cannot be considered either a field-related operation or an object-related operation, but a hybrid operation. The inclusion of discrete objects in our system can be easily accomplished since they are also supported by the geo-atom theory. Thus, as future work we plan to develop a whole 3D GIS for the management, analysis and visualization of not only volumetric terrains but also discrete objects, extending the theoretical model presented for terrains in this paper, to be able to deal with problems involving hybrid data. Eventually, the system will be released as open source in order to benefit GIS professionals and geoscientists.

Furthermore, we can enhance our framework by allowing the representation of heterogeneous materials. Material distributions are in fact heterogeneous by its very

```
<SBRT:StackBasedTerrain>
    <domainSet>
        <SBRT:RegularGrid dimension="2">
            <CIS:Axis axisLabel="Lat" lowerBound="0" upperBound="2" resolution="1"/>
            <CIS:Axis axisLabel="Long" lowerBound="0" upperBound="1" resolution="1"/>
        </SBRT:RegularGrid>
    </domainSet>
    <metadata>
        <CIS:Extension materialSet="ground 0, water 1, undefined u"/>
    </metadata>

    <CIS:Partition>
        <CIS:EnvelopeByAxis>
            <CIS:axisExtent axisLabel="Lat" lowerBound="0" upperBound="1"/>
            <CIS:axisExtent axisLabel="Long" lowerBound="0" upperBound="1"/>
        </CIS:EnvelopeByAxis>

        <coverage>
            <domainSet>
                <SBRT:IrregularGrid dimension="1">
                    <CIS:DistortedAxis>
                        <CIS:Axis axisLabel="Height" lowerBound="0" upperBound="5"/>
                        <CIS:Displacement directPosition="0, 2.5"/>
                    </CIS:DistortedAxis>
                </SBRT:IrregularGrid>
            </domainSet>
            <materialSet> 0 1 </materialSet>
            <GML:CoverageFunction>
                <sequenceRule> Linear </sequenceRule>
                <startPoint> 0 </startPoint>
            </GML:CoverageFunction>
        </coverage>
    </CIS:Partition>

    <CIS:Partition>
    ...
    </CIS:Partition>

</SBRT:StackBasedTerrain>
```

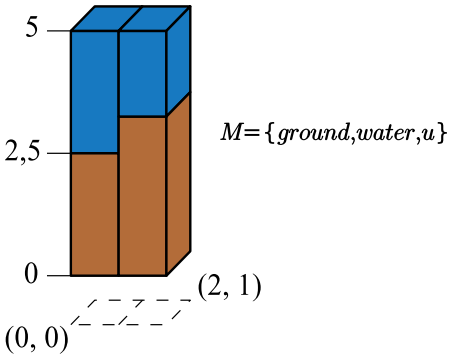

Figure 8. Use of GML for encoding a SBRT

nature since a material is usually mixed with those around it. For instance, in the transition between water and clay materials, there are points which present different proportions of them. The representation of this type of materials is a complex task since the proportions of the different mixes materials must be managed in a proper way. This feature would provide a more accurate representation and modeling of the strata at surface and subsurface levels.

References

Abedi, M., *et al.*, 2012. ELECTRE III: A knowledge-driven method for integration of geophysical data with geological and geochemical data in mineral prospectivity mapping. *Journal of Applied Geophysics*, 87, 9–18.

Arroyo Ohori, K., Ledoux, H., and Stoter, J., 2015. An evaluation and classification of n D topological data structures for the representation of objects in a higher-dimensional GIS. *International Journal of Geographical Information Science*, 29 (5), 825–849.

Benes, B. and Forsbach, R., 2001. Layered data representation for visual simulation of terrain erosion. *In*: *Proceedings Spring Conference on Computer Graphics*.

Billen, R. and Zlatanova, S., 2003. 3D spatial relationships model: a useful concept for 3D cadastre? *Computers, Environment and Urban Systems*, 27 (4), 411–425.

Borrmann, A. and Rank, E., 2009. Topological analysis of 3D building models using a spatial query language. *Advanced Engineering Informatics*, 23 (4), 370–385.

Brisson, E., 1993. Representing geometric structures in d dimensions: Topology and order. *Discrete & Computational Geometry*, 9 (1), 387–426.

Brooks, S. and Whalley, J.L., 2008. Multilayer hybrid visualizations to support 3D GIS. *Computers, Environment and Urban Systems*, 32 (4), 278–292.

Cacciari, P.P. and Futai, M.M., 2017. Modeling a Shallow Rock Tunnel Using Terrestrial Laser Scanning and Discrete Fracture Networks. *Rock Mechanics and Rock Engineering*.

Caumon, G., *et al.*, 2012. 3D implicit stratigraphic model building from remote sensing data on tetrahedral meshes: theory and application to a regional model of La Popa Basin, NE Mexico. *IEEE Transactions on Geoscience and Remote Sensing*, 51 (3), 1613–1621.

Čomić, L., *et al.*, 2014. Topological modifications and hierarchical representation of cell complexes in arbitrary dimensions. *Computer Vision and Image Understanding*, 121, 2–12.

Coors, V., 2003. 3D-GIS in networking environments. *Computers, Environment and Urban Systems*, 27 (4), 345–357.

Cordeiro, J.P.C., *et al.*, 2009. Yet another map algebra. *GeoInformatica*, 13 (2), 183–202.

Cova, T.J. and Goodchild, M.F., 2002. Extending geographical representation to include fields of spatial objects. *International Journal of Geographical Information Science*, 16 (6), 509–532.

Crespin, B., *et al.*, 2014. Generalized maps for erosion and sedimentation simulation. *Computers & Graphics*, 45, 1–16.

De Floriani, L., *et al.*, 2015. Morse complexes for shape segmentation and homological analysis: discrete models and algorithms. *Computer Graphics Forum*, 34 (2), 761–785.

de la Losa, A. and Cervelle, B., 1999. 3D Topological modeling and visualisation for 3D GIS. *Computers & Graphics*, 23 (4), 469–478.

de Oliveira Miranda, A.C., *et al.*, 2014. Finite element mesh generation for subsurface simulation models. *Engineering with Computers*, 1–20.

DeMers, M., 2002. *GIS Modeling in Raster*. Wiley.

Egenhofer, M.J., 1989. *A formal definition of binary topological relationships*. Berlin, Heidelberg: Springer Berlin Heidelberg, 457–472.

Egenhofer, M.J. and Franzosa, R.D., 1991. Point-set topological spatial relations. *International journal of geographical information systems*, 5 (2), 161–174.

ESRI. Environmental Systems Research Institute, 2017. ArcGIS, [`http://www.esri.com/`

arcgis/about-arcgis].
Forman, R., 1998. Morse Theory for Cell Complexes. *Advances in Mathematics*, 134 (1), 90–145.
Goodchild, M.F., 1992. Geographical data modeling. *Computers and Geosciences*, 18 (4), 401–408.
Goodchild, M.F., *et al.*, 1999. Introduction to the Varenius project. *International Journal of Geographical Information Science*, 13 (8), 731–745.
Goodchild, M.F., Yuan, M., and Cova, T.J., 2007. Towards a general theory of geographic representation in GIS. *International Journal of Geographical Information Science*, 21 (3), 239–260.
Graciano, A., Ruiz, A.J.R., and Higueruela, F.R.F., 2017. Real-time visualization of 3d terrains and subsurface geological structures. *Advances in Engineering Software (In press)*.
GRASS Development Team, 2016. Geographic resources analysis support system (grass gis) software, version 7.0. Available from: http://grass.osgeo.org.
Guo, J., *et al.*, 2016. Towards Automatic and Topologically Consistent 3D Regional Geological Modeling from Boundaries and Attitudes. *ISPRS International Journal of Geo-Information*, 5 (2), 17.
Hnaidi, H., *et al.*, 2010. Feature based terrain generation using diffusion equation. *Computer Graphics Forum*, 29 (7), 2179–2186.
Hollt, T., *et al.*, 2012. SeiVis: An Interactive Visual Subsurface Modeling Application. *IEEE Transactions on Visualization and Computer Graphics*, 18 (12), 2226–2235.
Hughes, J.F., *et al.*, 1990. *Computer Graphics: Principles and Practice*. 3rd ed. Boston, MA, USA: Addison-Wesley Professional.
Jjumba, A. and Dragićević, S., 2015. Towards a voxel-based geographic automata for the simulation of geospatial processes. *ISPRS Journal of Photogrammetry and Remote Sensing*, 117, 206–216.
Karimipour, F., Delavar, M.R., and Frank, A.U., 2010. A simplex-based approach to implement dimension independent spatial analyses. *Computers & Geosciences*, 36 (9), 1123–1134.
Kjenstad, K., 2013. On the hyperfield or field-of-field concept. *International Journal of Geographical Information Science*, 27 (5), 963–985.
Koca, Ç. and Güdükbay, U., 2014. A hybrid representation for modeling, interactive editing, and real-time visualization of terrains with volumetric features. *International Journal of Geographical Information Science*, 28 (9), 1821–1847.
Le, H.H., *et al.*, 2013. An object-relational spatio-temporal geoscience data model. *Computers & Geosciences*, 57, 104–115.
Ledoux, H. and Gold, C.M., 2008. Modelling three dimensional geoscientific fields with the Voronoi diagram and its dual. *International Journal of Geographical Information Science*, 22 (5), 547–574.
Lemon, A.M. and Jones, N.L., 2003. Building solid models from boreholes and user-defined cross-sections. *Computers and Geosciences*, 29 (5), 547–555.
Liu, Y., *et al.*, 2008. Towards a General Field model and its order in GIS. *International Journal of Geographical Information Science*, 22 (6), 623–643.
Löffler, F., Müller, A., and Schumann, H., 2011. Real-time Rendering of Stack-based Terrains. *Vmv*.
Longley, P.A., *et al.*, 2015. *Geographic Information Systems and Science*. 4th ed. Wiley Publishing.
Luricich, F. and De Floriani, L., 2014. A combined geometrical and topological simplification hierarchy for terrain analysis. *In*: *Proceedings of the 22nd ACM SIGSPATIAL International Conference on Advances in Geographic Information Systems - SIGSPATIAL '14*, nov, New York, New York, USA. ACM Press, 493–496.
Mateo Lázaro, J., *et al.*, 2014. 3D-geological structures with digital elevation models using GPU programming. *Computers & Geosciences*, 70, 138–146.
Maxelon, M., *et al.*, 2009. A workflow to facilitate three-dimensional geometrical modelling of complex poly-deformed geological units. *Computers & Geosciences*, 35 (3), 644–658.

Mennis, J., Viger, R., and Tomlin, C.D., 2005. Cubic Map Algebra Functions for Spatio-Temporal Analysis. *Cartography and Geographic Information Science*, 32 (1), 17–32.

Mitasova, H., *et al.*, 2012. Scientific visualization of landscapes and landforms. *Geomorphology*, 137 (1), 122–137.

Molenaar, M., 1992. A topology for 3D vector maps. *ITC Journal*, 1992-1, 25–33.

Molenaar, M., 1990. A formal data structure for 3D vector maps. *In*: *Proceedings of EGIS'90, Vol. 2*, Amsterdam, The Netherlands. 770–781.

Natali, M., Klausen, T.G., and Patel, D., 2014. Sketch-based modelling and visualization of geological deposition. *Computers and Geosciences*, 67, 40–48.

Noguera, J.M., *et al.*, 2011. Navigating large terrains using commodity mobile devices. *Computers and Geosciences*, 37 (9), 1218–1233.

OGC, 2003. *Geographic information — Spatial schema*. International Standard Organization.

OGC, 2007a. *OpenGIS ® Geography Markup Language (GML) Encoding Standard*. Open Geospatial Consortium Inc.

OGC, 2007b. *The OpenGIS ® Abstract Specification*. Open Geospatial Consortium Inc.

OGC, 2015. *OGC ® Coverage Implementation Schema Contents*. Open Geospatial Consortium Inc.

Ortega, L. and Rueda, A., 2010. Parallel drainage network computation on CUDA. *Computers and Geosciences*, 36 (2), 171–178.

Penninga, F. and Van Oosterom, P.J.M., 2008. A simplicial complex-based DBMS approach to 3D topographic data modelling. *International Journal of Geographical Information Science*, 22 (7), 751–779.

Peytavie, A., *et al.*, 2009. Arches: A framework for modeling complex terrains. *Computer Graphics Forum*, 28 (2), 457–467.

Pilouk, M., 1996. *Integrated modelling for 3D GIS*. Thesis (PhD). ITC, The Netherlands.

Ritter, G.X., Wilson, J.N., and Davidson, J.L., 1990. Image algebra: An overview. *Computer Vision, Graphics and Image Processing*, 49 (3), 297–331.

Rueda, A., Noguera, J.M., and Martínez-Cruz, C., 2013. A flooding algorithm for extracting drainage networks from unprocessed digital elevation models. *Computers and Geosciences*, 59, 116–123.

Schmitz, O., *et al.*, 2013. Map algebra and model algebra for integrated model building. *Environmental Modelling and Software*, 48, 113–128.

She, J. and Li, X., 2016. Map algebra based analysis for directed flow networks. *Transactions in GIS*, 20 (3), 356–367.

Shen, D., *et al.*, 2013. An ArcScene plug-in for volumetric data conversion, modeling and spatial analysis. *Computers & Geosciences*, 61, 104–115.

Shi, W., Yang, B., and Li, Q., 2003. An object-oriented data model for complex objects in three-dimensional geographical information systems. *International Journal of Geographical Information Science*, 17 (5), 411–430.

Takeyama, M., 1997. Building spatial models within GIS through Geo-Algebra. *Transactions in GIS*, 2 (3), 245–256.

Takeyama, M. and Couclelis, H., 1997. Map dynamics: integrating cellular automata and GIS through Geo-Algebra. *International Journal of Geographical Information Science*, 11 (1), 73–91.

Thiele, S.T., *et al.*, 2016. The topology of geology 1: Topological analysis. *Journal of Structural Geology*, 91, 27–38.

Tomlin, C.D., 1990. *Geographic information systems and cartographic modeling*. Prentice Hall series in geographic information science. Prentice Hall.

Voudouris, V., 2010. Towards a unifying formalisation of geographic representation: the object–field model with uncertainty and semantics. *International Journal of Geographical Information Science*, 24 (12), 1811–1828.

Wang, C., Wan, T.R., and Palmer, I.J., 2010. Urban flood risk analysis for determining optimal flood protection levels based on digital terrain model and flood spreading model. *The Visual Computer*, 26 (11), 1369–1381.

Wang, J., Duckham, M., and Worboys, M., 2015. A framework for models of movement in geographic space. *International Journal of Geographical Information Science*, 8816 (May), 1–23.

Wang, Z., *et al.*, 2016. Formal representation of 3D structural geological models. *Computers & Geosciences*, 90, 10–23.

Watson, C., *et al.*, 2015. Improving geological and process model integration through TIN to 3D grid conversion. *Computers & Geosciences*, 82, 45–54.

Wu, L., 2004. Topological relations embodied in a generalized tri-prism (GTP) model for a 3D geoscience modeling system. *Computers & Geosciences*, 30 (4), 405–418.

Yalçin, M.A., Weiss, K., and Floriani, L.D., 2011. GPU Algorithms for Diamond-based Multiresolution Terrain Processing. *In*: *Eurographics Symposium on Parallel Graphics and Visualization*. The Eurographics Association.

Yu, Z., *et al.*, 2016. Geometric Algebra Model for Geometry-oriented Topological Relation Computation. *Transactions in GIS*, 20 (2), 259–279.

Yuan, L., *et al.*, 2012. Geometric Algebra for Multidimension-Unified Geographical Information System. *Advances in Applied Clifford Algebras*, 23 (2), 497–518.

Yuan, L., *et al.*, 2014. Multidimensional-unified topological relations computation: a hierarchical geometric algebra-based approach. *International Journal of Geographical Information Science*, 28 (12), 2435–2455.

Zawadzki, T., Nikiel, S., and Warszawski, K., 2012. Hybrid of Shape Grammar and Morphing for Procedural Modeling of 3D Caves. *Transactions in GIS*, 16 (5), 619–633.

Zeiler, M., 1999. *Modeling Our World: The ESRI Guide to Geodatabase Design*. ESRI Press.

Zhao, Y., Padmanabhan, A., and Wang, S., 2013. A parallel computing approach to viewshed analysis of large terrain data using graphics processing units. *International Journal of Geographical Information Science*, 27 (2), 363–384.

Zhu, R., Kyriakidis, P.C., and Janowicz, K., 2017. *Beyond Pairs: Generalizing the Geo-dipole for Quantifying Spatial Patterns in Geographic Fields*. Cham: Springer International Publishing, 331–348.

Zlatanova, S., 2000. *3D GIS for urban development*. Thesis (PhD). ITC, The Netherlands.